DATA COLLECTION AND ANALYSIS

A tool to choose the Energy System and dimension the vehicle fleet of CTS systems

---

Deliverable Type: **REPORT**
Number: **D4.2**
Nature: **Final**
Contractual Date of Delivery: **August 2004**
Actual Date of Delivery: **December 2004**
WP4: City Experimentations
T4.2 Data collection and analysis

Name of responsible: **Prof. Yoram Zvirin**
Name of the institute: **TRI**
Technion – Israel Institute of Technology
Transportation Research Institute
Technion City, Haifa 32000
Israel

Abstract:

This document presents the work conducted within the framework of WP4 of the CyberMove Project: "Data Collection and Analysis". Data and simulation results of several cybercars and driving patterns are presented for four sites: INRIA Test Site, Technion Campus, RIVIUM–2 Loop and Antibes Route.
A theoretical model for simulating the performance of cybercars was developed, in order to calculate the energy consumption of the vehicle and the Cybernetic Transportation System (CTS). The simulation results obtained for any system under design can be used for comparison between various options of the vehicles power train. This enables to select its optimal components, like rated (or maximal) motor power, battery weight, etc. In addition, the driving pattern can also be devised for optimal energy consumption and driving range. The results presented here include daily energy consumption and recovery (by regeneration during braking) of the vehicles for the four sites mentioned above, and parametric studies of the effects of various vehicle and driving pattern data. Statistics analysis, calculations of daily energy consumption in dependence of season and comparison of ex-ante evaluation with ex-post simulations, which differ by CTS track length, number of stations, maximal and average car speed and acceleration for the Antibes site are presented. A comparison of the simulation results for the Antibes Route by the three Partners TNO, DITS and TRI shows quite close values for the energy consumption. The energy impact is discussed, based on the evaluation of the results.
The work described here has been carried out by the Consortium partners: TRI, INRIA, YME, FROG, TNO and DITS.

Keyword List: Cybernetic Transport System (CTS), CyberMove, CyberCars, OD pairs, Simulation Statistics, Energy Consumption, Numerical Calculations, Regeneration Braking.


CyberMove

Foreword

This deliverable was drafted under the responsibility of TRI (Transportation Research Institute of the Technion – Israel Institute of Technology.
The scientific supervisor was Professor Yoram Zvirin (TRI), who co-ordinated the work of Dr. Boris Aronov, Dr. Shlomo Bekhor, Dr. Leonid Tartakovsky and Dr. Vladimir Baibikov.
The following partners have also made significant contributions:

Kerry Malone and Gerdien Klunder (TNO)

Dr. Adriano Alessandrini and Daniele Stam (DITS)

Henry Raekers (FROG)

Dr. Michel Parent and Georges Ouanounou (INRIA)

Tim Meisner (YME)

TABLE OF CONTENTS

EXECUTIVE SUMMARY

This document presents the work conducted within the framework of WP4 of the CyberMove Project: "Data Collection and Analysis". The work described in this Report has been carried out by the Consortium partners: TRI, INRIA, YME, FROG, TNO and DITS.

The main goal of the CyberMove Project is to demonstrate the effectiveness of Cybernetic Transport Systems (CTS's) in solving city mobility problems, proving that they have now reached high levels of reliability, safety and user friendliness. The effectiveness is expressed by several different features, including better service, mobility, availability and accessibility; advantageous energy and environmental impacts; and cost benefit, taking into account externalities. Most of these issues are presented in the CyberMove Deliverables D2.3a and D6.2b: Ex-Ante Evaluation Report, [Alessandrini, 2004a], and D2.3b and D4.3: Ex-Post Evaluation Report, [Alessandrini, 2004b]. In the present Report, the energy impacts are presented and discussed, in this context, namely – minimization of the energy consumption and maximization of the driving range. This would lead to better service and to lower costs.

Algorithms and models were developed by TNO, DITS and TRI to simulate the behaviour of a cyber car on the road and a CTS. The TNO and DITS model were employed for site simulations, and in particular the Antibes Route, where actual operation of CTS's was carried out during demonstrations in June 2004. The statistics analysis for the Antibes appear in [Alessandrini, 2004a, b], some of the main results are summarized in the present Deliverable, including demand patterns. The TRI model was employed here mainly for parametric studies, in order to identify ways to optimize CTS energy consumption and driving range.

A theoretical model for simulating the performance of cybercars was developed, in order to calculate the energy consumption of the vehicle and the CTS. Data and simulation results of several cybercars and driving patterns are presented for four sites: INRIA Test Site, Technion Campus, RIVIUM–2 Loop and Antibes Route. The results obtained for any system under design can be used for comparison between various options of the vehicles power train. This enables to select its optimal components, like rated (or maximal) motor power, battery weight, etc. The results include daily energy consumption and recovery (by regeneration during braking) of the vehicles for the four sites mentioned above, and parametric studies of the effects of various vehicle and driving pattern data. Statistics analysis, calculations of daily energy consumption in dependence of season and comparison of ex-ante evaluation with ex-post simulations, which differ by CTS track length, number of stations, maximal and average car speed and acceleration for the Antibes site are presented. The energy impact is discussed, based on the evaluation of the results.

The main conclusion emerging from the simulation results is, indeed, that the CTS energy consumption can be minimized by careful design and choice of optimal parameters of both the vehicle and the driving pattern. It has been demonstrated that the functions of energy consumption, driving range and vehicle (or system) productivity (or number of passengers moved) have extrema at certain values of the battery weight, the maximal (or rated) motor power and the average vehicle speed (which represent the driving pattern, i.e. accelerations / decelerations). The importance of regenerative braking for energy conservation and increase of the driving range is also depicted.

The results presented in this report clearly show that it is possible to design the CTS and its operational procedure such as to offer better service and to minimize energy consumption.

1. INTRODUCTION

The main goal of the CyberMove Project is to demonstrate the feasibility of automated cybercar systems, or cybernetic transportation system (CTS's) in urban or private environments. It is co-funded under the City of Tomorrow Key Action of DG TREN Research Programme.

The potential advantages of autonomous driving capabilities and the new transport systems, based on environment friendly vehicles, are numerous, as elaborated in [Alessandrini, 2004b]. These include reduction of congestion, better mobility, accessibility and safety, improved air quality and optimized energy conservation. The latter issue is the subject of the present Report: the energy impact of the CTS.

This document presents the work conducted within the framework of WP4 of the CyberMove Project: "Data Collection and Analysis". Data and simulation results of several cybercars and driving patterns are presented for four sites: INRIA, RIVIUM–2, Antibes and Technion.

Theoretical model for simulating the performance of cybercars were developed by the three Partners TNO, DITS and TRI, in order to calculate the energy consumption of the vehicle and the CTS. The results obtained for any system under design can be used for comparison between various options of the vehicles power train. This enables to select its optimal components, like rated (or maximal) motor power, battery weight, etc. The results presented here include daily energy consumption and recovery (by regeneration during braking) of the vehicles for the four sites mentioned above, and parametric studies of the effects of various vehicle and driving pattern data. Statistics analysis, calculations of daily energy consumption in dependence of season and comparison of ex-ante evaluation with ex-post simulations, which differ by CTS track length, number of stations, maximal and average car speed and acceleration for the Antibes site are presented. The energy impact is discussed, based on the evaluation of the results. A comparison of the simulation results by the three Partners TNO, DITS and TRI for the Antibes Route shows quite close values for the energy consumption. The energy impact is discussed, based on the evaluation of the results.

The work described here has been carried out by the Consortium partners: TRI, INRIA, YME, FROG, TNO and DITS.

2. PERFORMANCE EVALUATION OF ELECTRIC VEHICLE

The present Chapter summarizes the research work on evaluation of the performance of cybernetic transportation systems (CTS), based on their behaviour on driving cycles. A theoretical study was developed for a general case of using two different energy sources for the propulsion system. The version described here is intended for a system using two types of batteries: a main one with large energy density and an auxiliary one with a large power density and capability of energy storage (regeneration) during braking. The theoretical results are in a good agreement with accessible experimental data. An investigation of regenerative braking efficiency for various driving conditions is also presented. Optimal values of variable parameters: the vehicle motor power, average speed, battery weight - are obtained for test sites.

Theoretical study of the two batteries case based on using of a battery with a high energy density as a main one (for example, Zinc-Air battery) and an auxiliary battery with a high power density. At least one of those batteries has to allow electrical recharging. The Zinc-Air battery that is being developed by Electric Fuel Ltd (EFL) is one of the advanced technologies under development today ([Harats et al, 1995]). Its energy density is more than 200 Wh/kg and the power density is of acceptable level – about 100 W/kg. The EFL concept of automotive Zinc-Air battery requires development of three linked systems:

1. On-board discharge-only battery pack.
2. Refuelling stations for fast and convenient mechanical exchange of consumed oxidized Zn electrodes with fresh ones.
3. Regeneration center for centralized recycling of oxidized Zn electrodes with well approved and environmental friendly Zn recovery technology.

Due to the fact that a Zn-Air battery has relatively low power density and cannot be recharged directly, an auxiliary rechargeable battery of relatively high power density is desirable. The auxiliary battery has to enable regenerative braking, which will lead to the reduction of energy consumption and to the increase in service life of the conventional vehicle brakes. Batteries with the required power density are now available; for example, Ni-Cd of 215 W/kg.

The configuration of the CTS propulsion system should be optimized, in order to allow minimal vehicle mass and optimal performance in the wide range of operation regimes and conditions. For this purpose, a simulation model was developed, which includes analytical dependencies of the efficiencies of the motor and batteries (main and auxiliary) in two operational modes: driving and regenerative braking. It is based on the mechanical equations of vehicle movement and takes into account heat losses in the electrical circuits. The main parameters of the model are: depth of discharge (DOD) of the batteries and the load factor of the motor, defined as the ratio of the traction power to its maximal value (for a given motor). The latter appears in the heat losses equation as an independent variable. The algorithm is used for calculation of the energy consumption, recoverable energy in the regenerative braking operation, etc. The expressions for the efficiencies are based on literature data and on measurement results described hereafter.

The model enables simulation of the control algorithm, which activates the auxiliary battery in cases where the available power of the main battery is too low compared to the needed traction power. It is assumed that an electrical coupler connects two energy sources in such a way that each one contributes its optimal power. A significant advantage of the model proposed here is that it requires a relatively small number of input parameters. Furthermore, it is rather simple and therefore user friendly, but it does have a certain limitation of accuracy. The latter is stipulated also by the lack of a complete data set, such as dependencies on the load factor of the driving and regenerative efficiencies

of the inverter, transmission, and of other details of real world driving conditions. Nevertheless, the simulation results obtained here are in good agreement with the experimental data.

2.1 THEORETICAL MODEL

A theoretical model was developed for evaluating the performance of electric vehicles equipped by a battery with large energy density (main) or by a combination of such a main battery and an auxiliary one with large power density and a regeneration braking capability. The model can be used for optimization of the battery block and of the power train parameters. It includes the relations between the electrical motor efficiency and load factor, between the batteries efficiencies and depths of discharging (DOD) for driving and regenerative braking (RB) operation (the RB – for the motor and the auxiliary battery only). These analytical relations have been derived in the present research work; their form and the set of needed input parameters are based on available literature data and on measurements performed in this work. Known mechanical equations and expressions for the heat losses in the electrical circuit have been used too. The latter relation involves the load factor as an independent variable and is obtained based on the known electro-dynamic relations. The model does not presuppose using large data files for efficiencies: of the vehicle motor η_{mot}, of the transmission η_{tr}, of the inverter η_{i}, of the battery η_{bat}, and for driving and RB operational conditions of the engine. The model uses empirical equations for the vehicle motor and battery efficiencies. The following assumptions have been adopted:

i) Transmission efficiencies: $\eta_{tr.dr}$, $\eta_{tr.reg}$, under driving and RB operation conditions, respectively, and that of the inverter: $\eta_{i.dr}$, $\eta_{i.reg}$ – are taken as mean values.

ii) For transient operation regimes the mean total RB efficiency, as well as the mean total of the reciprocal value of the driving efficiency, were calculated as functions of the load factor $P_{load} = P_{tr} / P_{tr.\max}$ at constant DOD (here: P_{tr} - traction power, $P_{tr.\max}$ - maximal traction power). The power in this case is approximately proportional to the vehicle speed at small low aerodynamic resistance (less than the acceleration force together with climbing and rolling forces). This is typical for electric vehicles.

iii) An effective ohmic load resistance is used in the calculations of heat losses in the electrical circuit of the vehicle. The mechanical equations with the corresponding empirical parameters are taken from the handbook ([Bosch, 1996]) and from [SIMPLEV, 2000]. The latter is used to account for the effect of the wind direction and speed on the aerodynamic drag coefficient.

iv) The vehicle route is divided into segments such that on each segment the vehicle speed and/or acceleration and the road gradient are constant.

2.2 MOTOR AND BATTERY EFFICIENCIES

As mentioned above, the theoretical model and the computer code enable, with a reasonable approximation, calculation of the motor and battery efficiencies, based on minimal input data by means of empirical equations. The latter are derived from published data in the form of the corresponding curves. Some parameters for these equations are obtained from measurements carried out previously by [Kottick et al, 2000]. The dependence of the motor driving efficiency, $\eta_{mot.dr}$, on the motor speed, N, in Fig. 1, as well as those of battery charge and discharge efficiencies, $\eta_{bat.reg}$, $\eta_{bat.dr}$, on the DOD in Fig. 2, have the same general form.

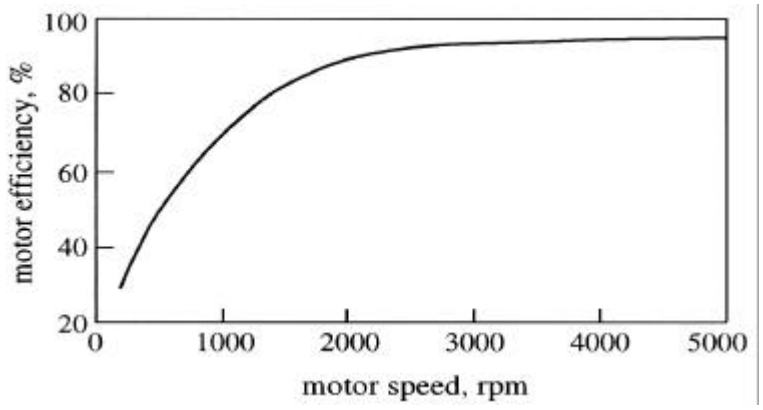

Fig. 1. Electric motor efficiency as a function of motor speed [Ehsani et al, 1999].

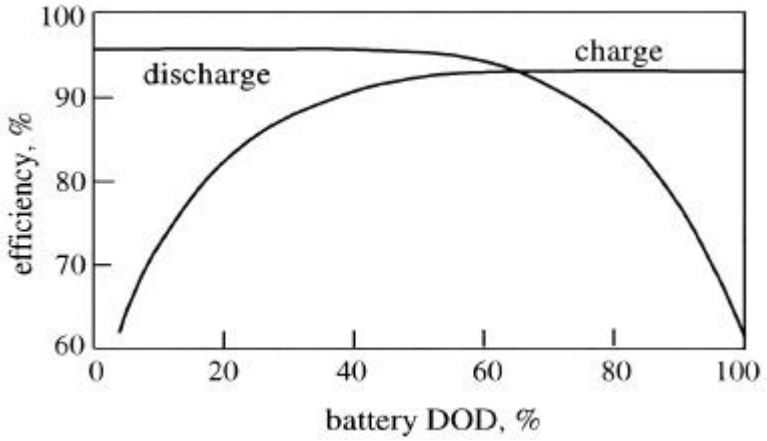

Fig. 2. Typical battery efficiency as a function of the depth of discharge for charge during regenerative braking, and discharge operation [Hochgraf et al, 1996].

An essential difference between the motor and battery efficiency curves (Figs. 1 and 2) is that the former represents dependence on the motor speed, N, rather than on a dimensionless parameter, i.e., the load factor, P_{load}.

On the other hand, the desired function, $h_{mot.dr}\ (P_{load})$, involves a parabolic curve which changes to a moderate slope, as seen in Fig. 3. The efficiency curve obtained in this work is of the same form.

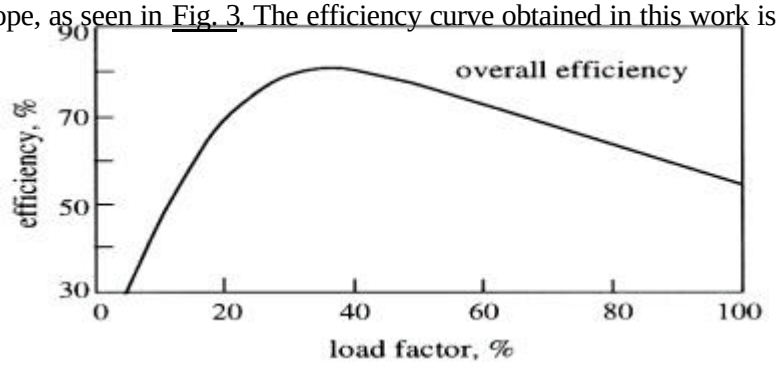

Fig. 3. Load factor effect on the overall electrical motor efficiency [Nicol and Rand, 1984].

The dependencies of the motor drive and regenerative efficiencies on P_{load} are written in the following form:

$$h_{mot}(P_{\text{load}}) = h^{0}_{mot}(P_{\text{load}}) * h_{heat}(P_{\text{load}}) \qquad (1)$$

Here the form of the basic motor efficiencies (without taking into account heat losses): $h^{0}{}_{\text{mot.dr}}(P_{\text{load}})$ and $h^{0}{}_{\text{mot.reg}}(P_{\text{load}})$, is the same as in Fig. 1 and the slope is determined by the heat losses efficiency, $h_{heat}(P_{load})$, associated with the ohmic losses in the electric propulsion system only. Since the efficiency curves of $h^{0}_{mot}(P_{load})$ and h_{bat} (DOD) have a similar shape, they can both represented by the same efficiency function, $h(P)$, with $P = P_{load} / P_{load\ max}$ for the case of motor efficiencies and P = DOD for the battery case:

$$h(P) = u \qquad \text{for} \quad P_{rel} = 0$$

$$h(P) = u * (1 - B * P_{rel}^{q}) \qquad \text{for} \quad P_{rel} > 0 \qquad (2)$$

$$B = (1 - \frac{l}{u}) / P_{rel.\max}^{q}$$

where u and l are the highest and lowest levels of the relevant efficiency in the corresponding range. For the efficiency curves (Figs. 1, 2), we define as D the value of the relative power or DOD, P, where the horizontal straight line is tangential to the sloped portion of the curve. For the motor efficiency and the battery charge efficiency, P_{rel} = D – P; for the battery discharge efficiency, P_{rel} = P – D. The parameters D and q, and the efficiencies of the motor and batteries under drive and regeneration braking operating conditions, are obtained from the curves in ([Ehsani et al, 1999]; [Hochgraf et al, 1996]), from data presented in [SIMPLEV, 2000], from three-dimensional diagram for h_{mot}(N, M) in [Caraceni et al, 1998] (where M is the motor torque), and from the experiments that were carried out by [Kottick et al, 2000]. The values of D and q are in the ranges:

0.3 = D = 0.5, 2 = q = 4,
while those of the upper and lower efficiency levels are in the ranges:

0.90 = U = 0.98, 0.25 = l_{mot} = 0.35, 0.5 = l_{bat} = 0.7.

It is obvious that the minimal regeneration braking efficiency for the auxiliary battery is zero. The regenerating efficiencies of the electric propulsion system components are lower than those in driving operation, cf. ([SIMPLEV, 2000]; [Hochgraf et al, 1996]; [Nicol and Rand, 1984]). This can serve as an indication for selecting the value of the regeneration efficiency in cases of lack of data.

Among the factors, which cause reduction of the regenerating efficiencies, the following two are of prime importance. During regenerative braking of electric vehicles, only the driven axle takes part in the process, while part of the braking energy is dissipated as heat by friction in the braking system of the non-driven axle. Therefore, the regenerative transmission efficiency is lower by approximately 10% than that in driving operation.

The total driving regenerative braking (RB) efficiencies and the corresponding energy consumption, E_{cons}, and regenerated energy, E_{reg}, are expressed by means of the following known equations:

$$h_{tot.dr} = h_{mot.dr} * h_{tr.dr} * h_{i.dr} * h_{bat.dr} \qquad (3a)$$

$$h_{tot.reg} = h_{mot.reg} * h_{tr.reg} * h_{i.reg} * h_{bat.reg} \qquad (3b)$$

$$E_{cons} = (P_{dr} / h_{tot.dr}) * t \qquad (3c)$$

$$E_{reg} = P_{dr} * h_{tot.reg} * t \qquad (3d)$$

Here t is the time, $h_{mot.dr}$ is given in eq. (1), $h_{tr.dr}$ is the transmission driving efficiency, $h_{i.dr}$ is the inverter driving efficiency, $h_{bat.dr}$ is the battery driving efficiency and similarly for the regenerating braking case. It is reminded that the heat losses factor, η_{heat}, also appears in eq. (1).

2.3 HEAT LOSSES IN ELECTRICAL CIRCUIT

As mentioned above, the assumption of an effective ohmic load resistance is adopted in the paper. Hence, heat losses in the battery and in electric conductors are:

$$P_{heat} = r_a I^2 \qquad (4)$$

where r_a is the ohmic resistance of the battery, and I is the electric current:

$$I = V_{oc}/(R+r_a) \quad (5)$$

where V_{oc} is voltage of the open circuit and R is load resistance. The outer power, $P_{out} = R*I^2$, takes the maximal value, P_{max}, at $R = r_a$, whence it follows:

$$r_a = \frac{V_{oc}^2}{4P_{\max}} \quad (6)$$

The heat losses efficiency, h_{heat}, in this approximation, is defined as:

$$h_{heat} = \frac{R}{R + r_a} \quad (7)$$

and P_{out} is given by:

$$P_{out} = R*(\frac{V_{oc}}{R + r_a})^2 \quad (8)$$

From equations (6-8) we obtain the following expression for the heat losses efficiency:

$$h_{heat} = \frac{1 - 0.5P_{out}/P_{\max} + \sqrt{1 - P_{out}/P_{\max}}}{1 + \sqrt{1 - P_{out}/P_{\max}}} \quad (9)$$

It is noted that here P_{out}/P_{max} is P_{load}. It is determined as a function of the drive power, P_{dr}, and of the corresponding efficiencies: η_{dr}^{ℓ}, $\eta_{bat.reg}$ and h_{reg}^{0}, for the drive and regenerative braking operations, respectively, with minimal drive efficiency, h_{dr}^{ℓ}, obtained experimentally, $h_{reg}^{o} = h_{mot.reg}^{o} * h_{tr.reg} * h_{i.reg}$. In the drive mode, the parameter $P = P_{load}$ is:

$$P = \frac{p_{dr}}{P_{\max} * h_{dr}^{l}} \quad (10)$$

where $P_{\max}$ is maximal motor power. In the regenerating braking mode:

$$P = P_{dr} * h_{reg}^{o} / (P_{bat.\max} * h_{bat.reg}) \quad (11)$$

where $P_{bat.\max}$ is the maximal battery power. If $P_{dr} * h_{reg}^{0}$ is larger than $P_{bat.\max} * h_{bat.reg}$, then the total RB efficiency is equal to:

$$h_{tot.reg} = \frac{P_{bat.\max} * h_{bat.reg}}{P_{dr}} \qquad (12)$$

2.4 MECHANICAL EQUATIONS

The expressions for the climbing resistance force, F_{cl}, rolling force, F_{rol}, and the acceleration force, F_{acc}, with the corresponding empirical coefficients, are taken from the handbook ([Bosh, 1996]):

$$F_{cl} = m * g * \sin a \qquad (13)$$

where m is the vehicle mass, g is the acceleration of gravity and a is the road gradient.

$$F_{rol} = C_1 * (1 + C_2 * v) * m * g * \cos a \qquad (14)$$

Here C_1 = 0.01; C_2 = 0.00447 s/m and v is the vehicle speed.

$$F_{acc} = k_r * m * a \qquad (15)$$

where a is the vehicle acceleration and $k_r = 1.03$ is the rotation coefficient.

The aerodynamic drag force, F_{drag}, is taken from [SIMPLEV, 2000]:

$$F_{drag} = \pm 0.5 C_d C_{cor} r_{air} A v_{rel.l}^2 \qquad (16)$$

where r_{air} is the air density, A is the maximal vehicle cross section, C_d is the drag coefficient (for a van it can be taken equal to 0.6), C_{cor} is a correction factor, accounting for the lateral component of the wind speed, $\vec{v}_w$, in relation to the vehicle speed, $\vec{v}$: $\vec{v}_{w.rel} = \vec{v}_w - \vec{v}$. It is determined as:

$$C_{cor} = 1 + a_1 |g|^b \quad \text{for } |g| < 17.5$$

$$C_{cor} = 1 + a_1 * 17.5^b \quad \text{for } |g| > 17.5 \qquad (17)$$

Here g is the angle between the directions of $\vec{v}$ and $\vec{v}_{w.rel} = \vec{v}_w - \vec{v}$, a_1 = 0.00194 and b = 1.657. The sign of F_{drag} in eq. (16) is determined by the sign of the longitudinal component of the relative speed between the vehicle and the wind, $\vec{v}_{rel} = \vec{v} - \vec{v}_w$, that is represented by $\vec{v}_{rel.l}$ in eq. (16). The acceleration time, t_{acc}, is calculated according to the known formula, e.g. in [Meier-Engel, 2000]:

$$t_{acc}=\int_0^{V_a} \frac{k_r m v * dv}{P_{dr.\max} - F_{st} v - C_{rol} v^2 - C_{aer} v^3} \qquad (18)$$

where n_a is the prescribed speed [km/h], attained by the vehicle for the acceleration time t_{acc} from the start, at the maximal drive power $P_{dr.max} = P_{bat.max}$*?$_{tot.dr}$, $P_{bat.max}$ is the battery power at relatively small DOD, $F_{st} = C_1 * m * g * \cos a$ is the first term in eq. (14) and

$C_{aer} = F_{drag} / v_{rel.l}^2$, with F_{drag} from eq. (16).

The set of mechanical equations (13 – 17) enables calculation of the acceleration, climbing, rolling and aerodynamic drag resistance forces. These are needed for further calculations of the driving and regeneration braking power, and energy consumed and saved, which are inversely and directly proportional to the corresponding total efficiencies of the electric vehicle propulsion system, respectively. The total efficiencies are products of the battery block, motor, inventor and traction efficiencies. The mean values of the latter two must be given in the input file. The previous two efficiencies are calculated according to the algorithm described above.

2.5. VALIDATION OF THE MODEL

Efficiency parameters that are used in the theoretical model were selected, in order to ensure the best possible correlation of simulation results with available experimental data.

Validation of the model was performed on the example of an electric vehicle (EV) of van type, for which detailed experimental data were available. An attempt to obtain an optimization of the weights of the main (Zinc-Air) and the auxiliary (Ni-Cd) batteries was undertaken under conditions of the constant vehicle speed and standard urban drive cycle. Some results are presented in figures 4 and 5.

As an example, a combined weight of the two battery types was taken as 1250 kg, and vehicle weight of 3500 kg. A driving range of 395 km was obtained for the main and auxiliary battery weights of 850 and 400 kg, respectively, and an optimal range of 515 km was found for weights of 1100 and 150 kg, respectively. An energy consumption of 0.460 kWh/km and regenerated energy of 0.032 kWh/km were obtained for the latter (optimal) case. Different driving styles were also investigated theoretically for the standard urban drive cycle and the same values of the efficiencies, total vehicle and the propulsion system weights. The above-mentioned results were obtained for the "normal" driving style. A maximal driving range of only 245 km was obtained for the "aggressive" style with an energy consumption of 0.585 kWh/km and main and auxiliary battery weights of 600 and 650 kg, respectively. Values of the same parameters for "calm" driving style are as follows: range of 755 km, energy consumption of 0.355 kWh/km, when the propulsion system includes a main battery only, of 1250 kg

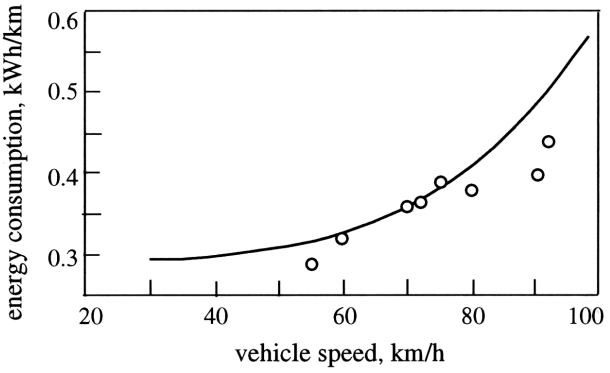

weight.

Fig. 4. Energy consumption - constant speed driving.

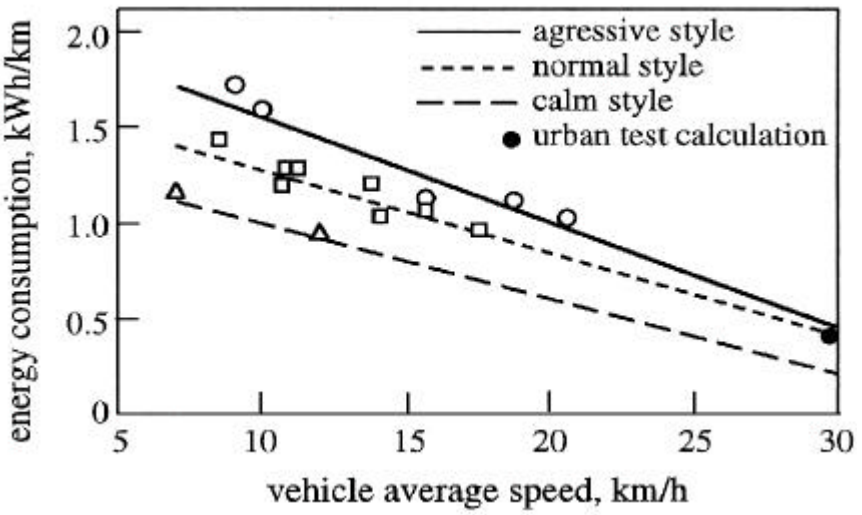

Fig. 5. Energy consumption - city center driving

The energy consumption for the normal driving style ranges from 0.9 kWh/km at an average speed of 20 km/h, to 1.4 kWh/km at an average speed of 8 km/h. The energy consumption in a congested city center cycle, where the driving has a stop-and-go nature, is drastically higher than at constant speed.

It is concluded that a reduction of at least 50% of the energy consumption can be reached when the driving pattern (and style) is optimized.

Acceleration time values were accounted for in the theoretical model for pre-selection of the overall efficiency at maximal loads and compared with the available statistical data.

The acceleration time of the EV when the battery was fully charged was 35.5 sec as compared to 38.1 sec when the battery's DOD was 50 % - an increase of only 7%. These results demonstrate that the dependency of the power density on the charging state of the battery is relatively weak in this range for the studied battery type.

3. DATA COLLECTION ON CYBERCARS AT SEVERAL SITES

The model presented in the previous Chapter was employed to simulate the behaviour of cybercars in four different sites: INRIA test site, the Technion Campus, the Rivium – 2 loop and the Antibes route. The data collected on vehicles parameters and driving patterns were based on information provided by the site responsibles and car manufacturers and operators. The main parameters are presented below for each of the four sites.

3.1 INRIA TEST SITE

A Yamaha – Europe (YME) vehicle, shown in Fig. 6, was tested in the loop (cycle) at the INRIA test site. It has been used for demonstrations as well as for tests.

Fig. 6. YME Vehicle at INRIA.

Simulated Vehicle

- Gross vehicle weight – 1250 kg
- Frontal area – 2.31 m^2
- Battery type – Lead-Acid
- Maximal DOD – 0.8
- Basic battery weight – 126 kg

Simulated Driving Pattern

- Driving route – INRIA testing route
- Route length – 555 m
- Road gradients – as were supplied by INRIA
- Driving cycle – as was experimentally measured by INRIA

- Basic average speed – 8.7 km/h

3.2 TECHNION CAMPUS

A CTS was pre-designed for the Technion (Israel Institute of Technology) Campus in Haifa. The simulations were performed for the YME vehicle described above, shown in Fig. 6. The route is shown in Fig. 7.

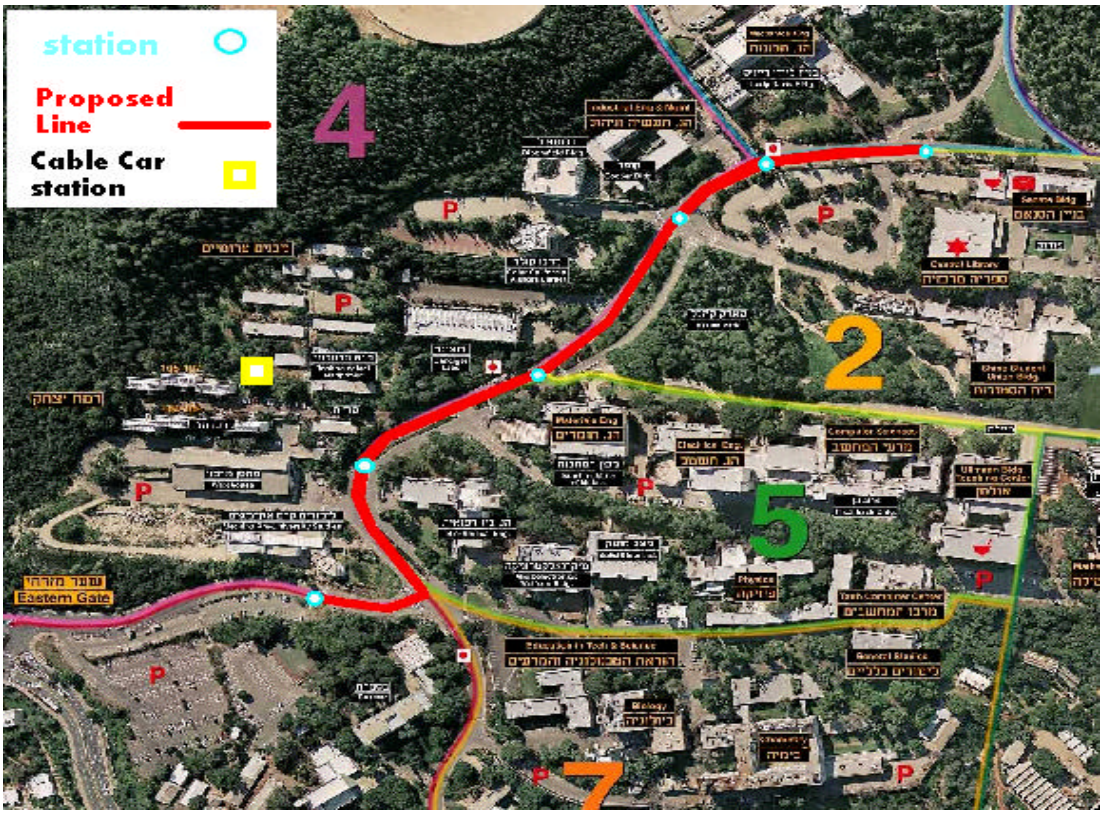

Fig. 7. The CTS route designed for the Technion Campus.

Simulated Vehicle

- Gross vehicle weight – 1250 kg
- Frontal area – 2.31 m^2
- Battery type – Lead-Acid
- Maximal DOD – 0.8
- Basic battery weight – 130 kg

Simulated Driving Pattern

- Driving route – Technion testing route

- Route length – 1600 m
- Absolute averaged value of the road gradients is 7.5%
- Driving cycle – as was experimentally measured by TRI
- Basic average speed – 12.0 km/h

3.2 RIVIUM - 2 LOOP

Rivium – 2, designed by FROG with their own vehicles (Fig. 8), is scheduled to start operation in the first half of 2005. It is an extension of an earlier system, Rivium – 1, which was operated as part of the Rotterdam public transportation system. The design figures of the FROG cyber vehicle were used in the simulations of the Rivium -2 loop.

Fig. 8. FROG vehicle in Rivium - 2

Simulated Vehicle

- Curb vehicle weight (incl. battery) – 4650 kg
- Passengers capacity – 20
- Frontal area – 5.78 m^2
- Battery type – Lead Acid
- Maximal road gradient – 5%
- Basic battery weight – 1450 kg

Simulated Driving Pattern

- Driving route – RIVIUM 2 site
- Total route length – 3.6 km
- Maximal road gradient – 5%

- Total number of stops – 10
- Basic average speed – 18 km/h

3.3 ANTIBES ROUTE

A cyber car that was used is similar to the one designed and manufactured by FROG for Rivium – 2. It was demonstrated in Antibes in June 2004. on the loop shown in Fig. 9.

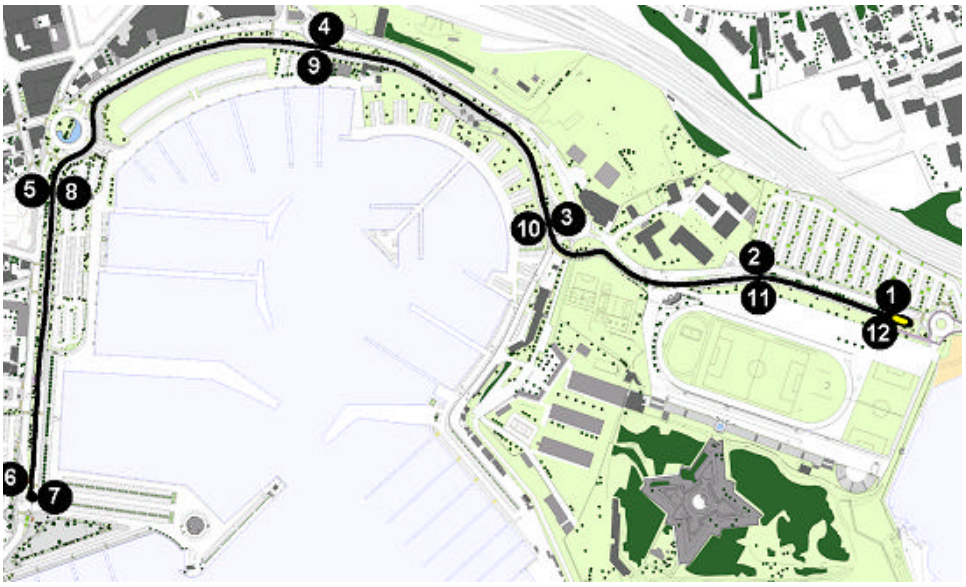

Fig. 9. The Antibes CTS route. The circles 1 – 4 represent vehicle crossings, the blue dots pedestrian crossings.

Simulated Vehicle

- Gross vehicle weight – 4650 kg
- Passengers capacity – 20
- Frontal area – 5.78 m2
- Battery type – Pb-Acid
- Maximal DOD – 0.8
- Basic battery weight – 1450 kg

Simulated Driving Pattern

- Driving route – Antibes testing route
- Route length – 2989 m
- Plain road
- Driving cycle – as experimentally measured in Antibes
- Basic average speed – 12.6 km/h

4. ANALYSIS OF DATA ON CYBER CARS

The simulation model was applied using the calculation procedure described below. The whole route of the vehicle is divided into N+1 sections (from 0 to N), with the following requirements:

a) The section can include segments of constant drive speed as well as of accelerated / decelerated drive, but the section is characterized by a single speed value and a single absolute value of acceleration (deceleration) in each segment.

b) The constant speed value, VC (m/s), is equal to that at the interface between the section of interest and the successive one. In the case of variable speed at the end of the section, a very short segment of constant speed is applied.

c) The road gradient and an angle of the travel direction are taken as constant values within the whole section length.

The section can include several stops, NST, and speed changes, NCH, with the same absolute value of the acceleration. 'Stop' is simply full stop of the vehicle, with subsequent return to the constant stationary drive speed for the section, VC, except for the last section (N), where NST = 1 and the final speed is equal to 0. 'Speed change' means that VC for the section changes at the section acceleration to another value (higher or lower than VC) with an immediate return to VC. In case of speed changes in a section, the same pattern was assumed of deceleration and than acceleration (or vice versa) to the constant representative speed.

As noted above, the algorithm can treat two energy sources for the propulsion system, for example a main battery with high energy density and an auxiliary one with high power density. The vehicles in the four sites had one battery only, so the simulations were performed with a simpler version.

The simulation algorithm and computer code take into account the dependence of the vehicle traction system efficiency on the traction power that depends in turn on the road gradients, the vehicle weight, cross section area, speed and acceleration (deceleration). The dependence of the electrical motor efficiency on the load factor and on the heat losses is taken into account also.

The simulation model was employed for a parametric study, in order to investigate the effects of the battery weight, the electric motor power and the average speed on the vehicle (or system) performance: driving range, energy consumption and number of passengers moved. For this we define the vehicle productivity as:

$$VP = PC*R$$

Where:
PC – passenger capacity of the vehicle
R – driving range between battery recharging, km

And number of passengers moved (NPM), for full capacity, as:

$$NPM = VP / L$$

Where:

L – route length, km

These definitions apply for a single vehicle on the route as well as for the whole CTS system.

The energy consumption and the driving range (directly related to it) can be calculated for any electric vehicle in any site (on any road or route). The results enable to optimize various parameters, and in particular the motor maximal power, the vehicle speed and driving pattern and battery weights. Furthermore, it is emphasized that the CTS has an inherent advantage in this respect of energy conservation, since it is operated without drivers, and thus the driving pattern can be programmed in an optimal manner. The results shown in fig. 5 clearly demonstrate it: the energy consumption strongly depends on the driver's driving style. Obviously, the CTS performance is independent of human behaviour on the road.

In the following results of the simulations are presented for the four sites – INRIA, Technion, Rivium – 2 and Antibes, according to the data collected and summarized in Chapter 3. For the Antibes site, a statistical analysis was performed including the total passenger-km travelled: per day, per day in peak hours, per day in off-peak hours; total number of one-way trips, and also for those starting in the above-listed hours; average vehicle occupancy over a day per unit of time and starting in these hours; number of km - empty vehicles over a day, and the influence of the season on these parameters.

4.1 INRIA TEST SITE

INRIA provided, tin addition to the data in Chapter 3, a map of the site with the corresponding road gradients and detailed drive parameters: the cyber car speed, distance travelled, etc., as functions of time, with time-step of 30 ms. Based on these data, the road was partitioned into 34 sections of the same speed, acceleration and speed change pattern for each of them.

The main simulation results are presented in the figures 10 - 14, for the data on the vehicle, road and driving pattern of Chapter 3.1. The parametric study is based on the input data.

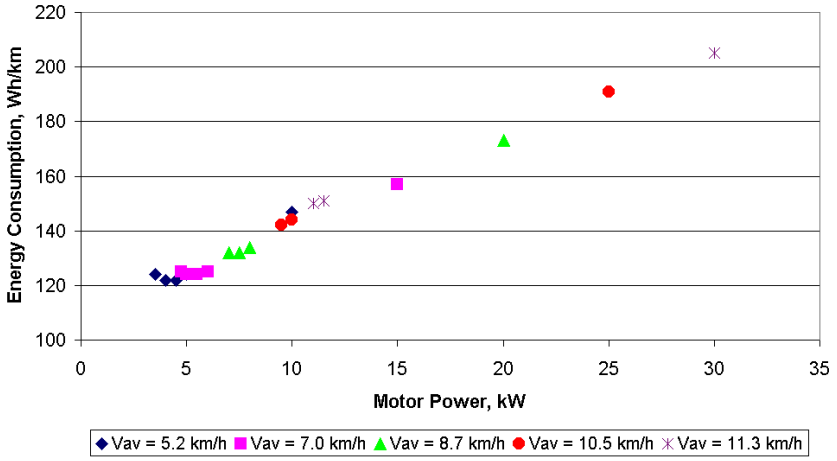

Fig. 10. Motor power effect on energy consumption.

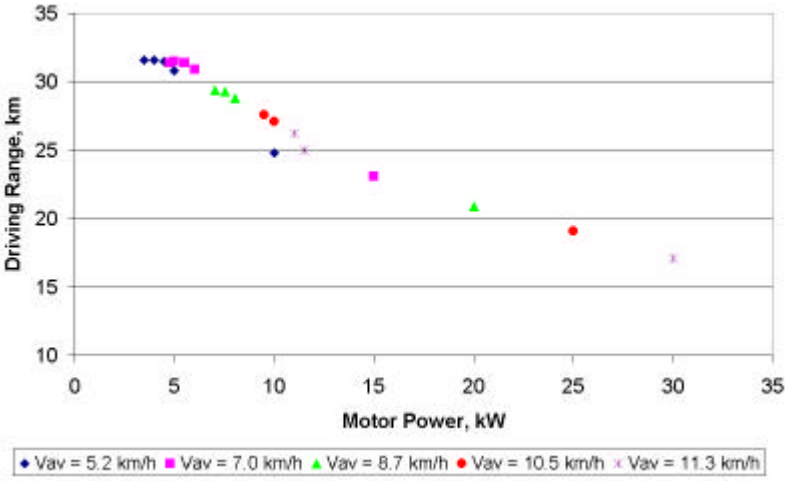

Fig. 11. Motor power effect on driving range.

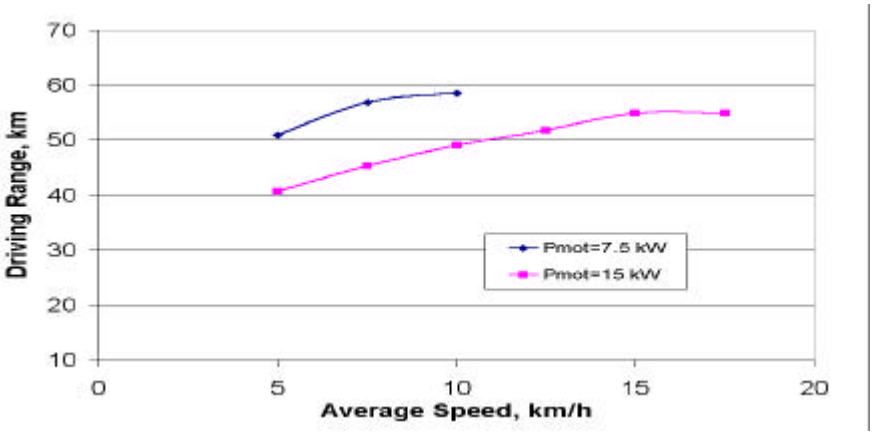

Fig. 12. Average speed effect on driving range.

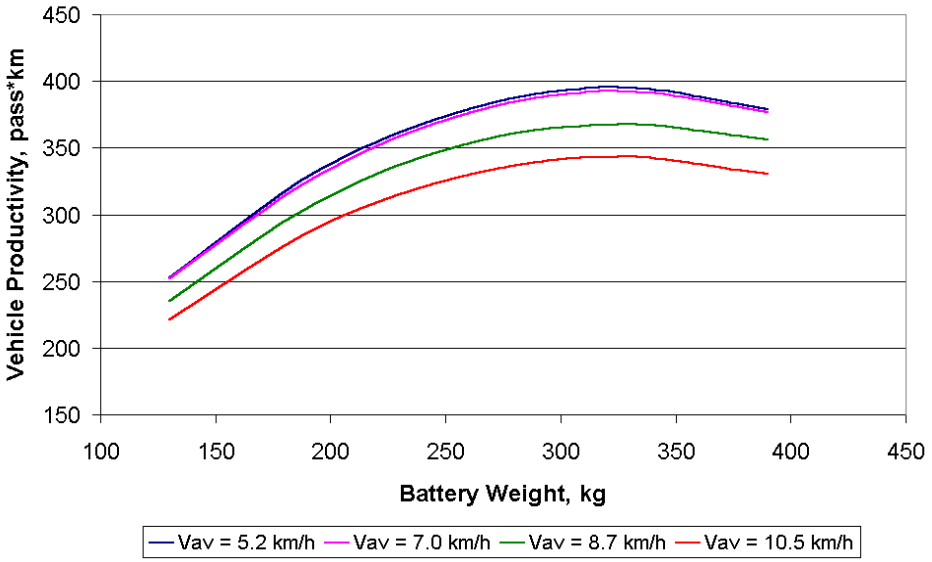

Fig. 13. Effects of battery weight and average speed on vehicle productivity.

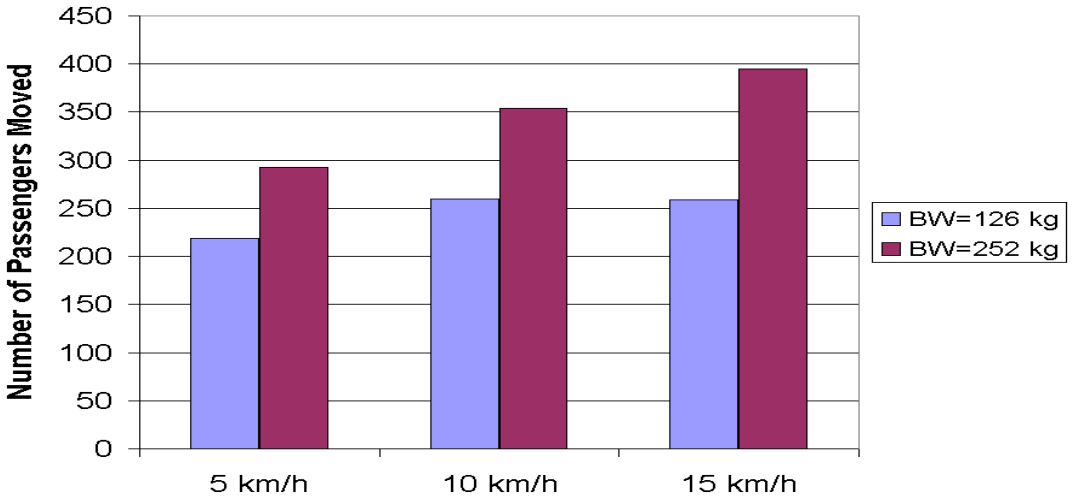

Fig. 14. Effects of battery weight and average speed on number of passengers moved.

It is immediately obvious from the results that the vehicle (or system) performance can be optimized: the energy consumption can be minimized, and the driving range can be maximized by selecting appropriate parameters such as battery weight, rated (or maximal) motor power and average vehicle speed. The latter must be chosen, of course, not only according to the energy considerations but also (and more importantly) to satisfy mobility and safety requirements, for example waiting times.

Figures 10 and 11 show the effects of the rated (or maximal) motor power on the energy consumption and the related driving range. The appearance of the curves is mainly due to the effects of the efficiencies of the propulsion system components. It can clearly be seen that by careful design and selection of the motor, considerable energy savings can be achieved, with an increase of the driving range. This is important also since it leads to better system availability during operation, associated with optimized system size (number of vehicles). Similarly, the driving pattern, represented here by the average velocity, has a strong impact on the energy consumption, as seen in Fig. 12. The effects of the battery weight and the average speed on the productivity and number of passengers moved are illustrated in Figs. 13 and 14. Again – the maxima of the various curves indicate clearly that optimization can be achieved, leading to significant energy savings, increased driving range and better system performance.

4.2 TECHNION CAMPUS

4.2.1 Technion Campus: Statistics Analysis

CTS Project Description

The objective of the CTS project is to improve the accessibility inside the Campus for two main populations:

- Students and visitors arriving by private car who park far from the main buildings.
- Public transport riders who have limited mobility inside the Campus, because of the long walking distances with slopes.

The project is divided into two main phases:

Phase 1: Connection between three big parking lots and some of the faculties in a linear line. Two of the parking lots are located close to the Eastern Gate, and the third one is near the main promenade. The line passes near the projected cable car station, which is also located near this gate. This phase is oriented to improve accessibility for students parking far from the main buildings.

The vehicles will have to travel alongside existing traffic. It will be possible to control all the intersections in order to avoid conflicts. The existing right of way comprises two lanes in each direction; one of them is generally used for parking, which could be adapted for the CTS vehicles. Therefore, the vehicles can run independently in both directions. At both ends of the line there is enough room to accommodate the vehicles (recharging, storing idle vehicles, etc).

Phase 2: Completion of the initial line to a closed loop that connects most of the faculties and public buildings. This phase is oriented to serve both populations listed above. The length of the loop is 2.4 km.

For the purpose of this research, the study was limited to Phase 1 only. Figure 7 shows an aerial photo of the Technion Campus with the proposed line.

Demand Forecast Estimation

To obtain an estimate of the demand for the proposed CTS line, an estimated logit model was used, based on a Stated Preference (SP) study performed in the campus. The statistics analysis for the

Technion Campus is included in the CyberMove Deliverable D2.3a and D6.2b: Ex- Ante Evaluation Report, [Alessandrini, 2004a]. The SP study is also described in detail in [Bekhor and Zvirin, 2004]. It was assumed that the CTS line would not attract new passengers, since it is mainly oriented to complement existing services.

The first step in the estimation was the calculation of probabilities of choosing alternative modes. For simplicity, we assumed four modes: bus, car (either driver or passenger), van and the new CTS mode. Using average values of 5 min travel time and 5 NIS travel cost, we calculated the probability of choosing each mode for each population segment. Table 1 summarizes the results.

Table 1. Mode Choice Results by Population Segment.

Population Segment (among students)	Proportion from total students	Probability of Choosing Each Mode			
		bus	car	van	CTS
Male, with car	32%	19%	33%	12%	36%
Female, with car	10%	23%	40%	15%	22%
Male, without car	35%	12%	21%	8%	59%
Female, without car	23%	17%	30%	11%	42%
All segments	100%	17%	29%	11%	44%

The second step in the estimation was the calculation of total trips for each mode. This step was accomplished using the origin-destination matrix, assuming the base case proportions (i.e., 30% bus, 51% car, 19% van). Since the proposed line is close to the Eastern Gate, and relatively far from the Western Gate, we assumed as potential trips all trips arriving from the Eastern Gate, and only 50% trips arriving from the Western Gate.

We also assumed that total trips of cars with parking permits will remain unchanged. This is consistent with the assumption that most students do not possess a parking permit. Therefore, they have the following options to arrive the Campus: car (without parking permit), bus or van. Table 2 summarizes the total number of trips estimated before and after the CTS line.

Table 2. Summary of Total Estimated Trips by Mode

Mode	Before CTS line				After CTS line			
	Vehicle-trips		Person-trips		Vehicle-trips		Person-trips	
	Western	Eastern	Western	Eastern	Western	Eastern	Western	Eastern
Car (without permit)	1682	472	2271	637	1607	14	2169	19
Car (with permit)	3934	1864	4524	2144	3934	1864	4524	2144
Bus	231	65	5775	1625	166	32	4154	806
Van	454	55	2270	275	391	104	1954	522

truck	60	61	60	61	60	61	60	61
CTS	0	0	0	0	340	198	2038	1191
Total	6361	2517	14900	4742	6497	2274	14900	4742

The results in Table 10 show that a total of 3,229 persons will ride the CTS line in an average weekday. Assuming an average of 6 persons travelling in each Cybercar, a total of 538 vehicle-trips are obtained.

The total mode share of the CTS system is 3,229/19,642 = 16%. Since we assumed that the total number of trips will remain unchanged, this means that the CTS system will reduce 720 person-trips by car, 2440 person-trips by bus and 69 person-trips by shuttle van.

4.2.2 Technion Campus: Energy Consumption Calculations

The Technion Campus data for the vehicle and route are given in Chapter 3. As mentioned above, the Campus is on a rather steep hill and the CTS would be attractive to passengers, who may use it instead of walking uphill (and downhill too). The average road gradient is 7.5%.

The simulation was performed separately for the two parts of the road – downhill and uphill. The results are shown in Fig. 19 and Tables 3 and 4. The effect of battery weight on the cyber car productivity was investigated and the results are presented in Fig. 19. It is clearly seen, as for the INRIA case presented above, that the curve for the number of passengers moved vs. the battery weight depicts a maximum, here – at 355 kg (for the specific vehicle, speed and route data). It is demonstrated, again, that the system can (and should) be designed such as to optimize it.
Results for the energy consumption and regeneration for the two road sections (downhill and uphill) and the whole route, at the average vehicle speed of 12 km/h, are presented in Table 11. It is noted that here a "hypothetical" vehicle was simulated, with the same shape (frontal area) and same total weight of the vehicle that was used and simulated at the INRIA site, but with various possible passengers' capacity. The results in the Table show that the optimal battery weight is 355 kg. Table 12 includes additional simulation results with this optimal weight (and 5 passengers in the vehicle). As can be seen, the regenerated energy on the downhill section is very significant. It is therefore emphasized that a regenerative braking system should be included, in order to save energy and to increase the driving range. This is an important part of the optimization design of the CTS.

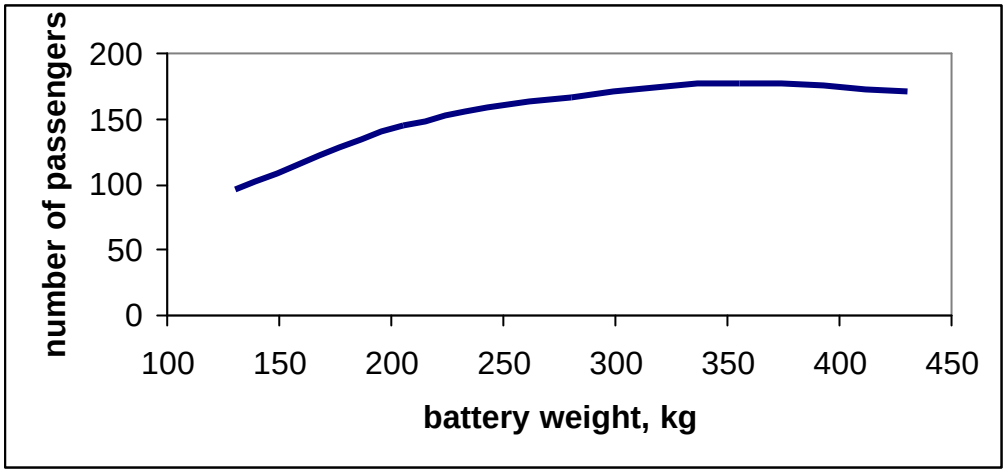

Fig. 19. Battery weight effect on number of passengers moved.

Table 3. Effects of Battery Weight and Vehicle Passenger Capacity on Energy Consumption and Regeneration and Driving Range.

	Simulation Experiment				
	1	2	3	4	5
Battery weight (kg)	130	205	280	355	430
Number of passengers in each car	8	7	6	5	4
Energy consumption per km (kWh/km)	0.229	0.215	0.218	0.217	0.219
Downward Energy consumption per km (kWh/km)	0.027	0.028	0.028	0.028	0.028
Upward Energy consumption per km (kWh/km)	0.465	0.414	0.422	0.414	0.418
Regenerated energy per km (kWh/km)	0.052	0.055	0.055	0.055	0.055
Drive range is equal to: (km)	19.2	33.1	44.6	57.1	68.6
Mean speed is: (km/h)	12.0	12.0	12.0	12.0	12.0
Total vehicle-trips for a single car	12	21	28	36	43
Total person-trips for a single car	96	145	167	178	172
Total person-trips needed	3229	3229	3229	3229	3229

Total cars needed to run the system	34	22	19	18	19
Total System Consumption (Wh)	147630	158493	188063	43508	94929

Table 4. Energy Consumed and Regenerated

5-Passenger case, battery weight	355 kG
Total energy consumption Energy consumption per km	124 kWh 0.217 kWh/km
Downward energy consumption Energy consumption per km	824 Wh 0.028 kWh/km
Upward energy consumption Energy consumption per km	11.5 kWh 0.414 kWh/km
Total regenerated energy Regenerated energy per km	3.15 kWh 0.055 kWh/km
Downward regenerated energy Regenerated energy per km	315 kWh 0.108 kWh/km
Drive range	57.1 km
Average speed	12 km/h

4.3 RIVIUM - 2 LOOP

The simulation model was employed to investigate the effects of the motor power, the battery weight, the average vehicle speed and the vehicle load (number of passengers) on the driving range and the

vehicle productivity for the RIVIUM - 2 site. Results for the energy consumption are not shown here – they are closely related to the driving range. The results, presented in Figs. 20 – 24, show similar trends as for the INRIA and Technion sites. The driving range decreases with the increase of the motor power (Figs. 20, 21), due to the behaviour of the of the propulsion system efficiency. Obviously, the driving range decrease when the vehicle carries more passengers. The driving range increases with average speed (Figs. 22, 23), mainly due to smaller number of accelerations at the higher average speeds. This effect is stronger when the route has fewer segments – less stops; the results in Fig. 23 represent a case of 10 segments, while those in the other figures here are for 16 segments. It is noted that at the speed range considered here, the drag forces are not very significant and may have some influence only at higher speed values and lower power. In the Antibes site, with a different driving pattern, a different trend was observed, as discussed below in Chapter 4.4.2.

Fig. 24 shows behaviour of the vehicle productivity under the influence of the battery weight, motor power and passenger number. It can be seen, similar to the results for the INRIA and Technion sites, that the vehicle productivity increases with up to some “optimal” value, and then starts to decrease.

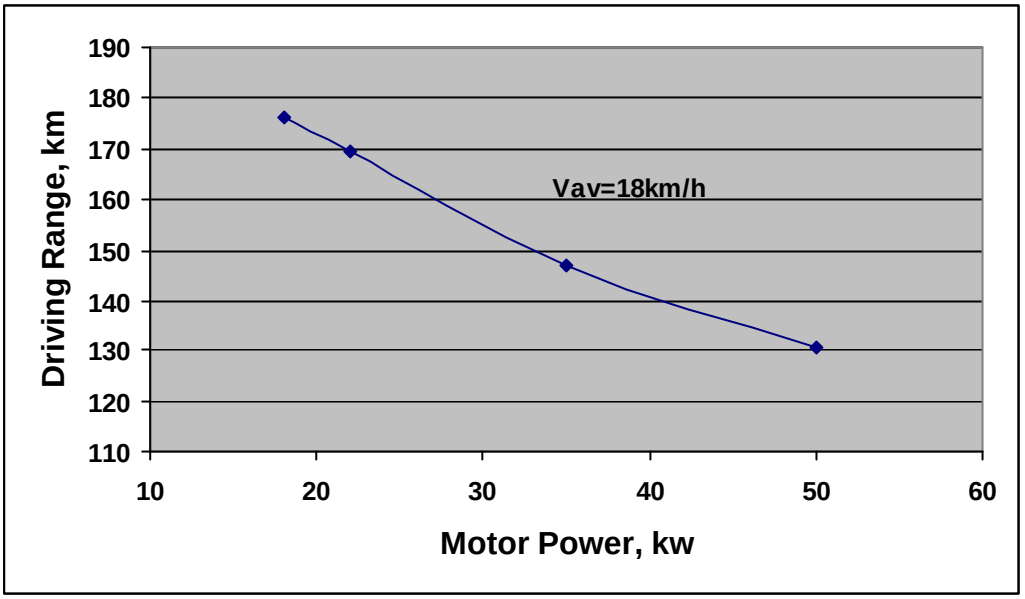

Fig. 20. Motor power effect on driving range, 6 passengers, average velocity 18 km/h.

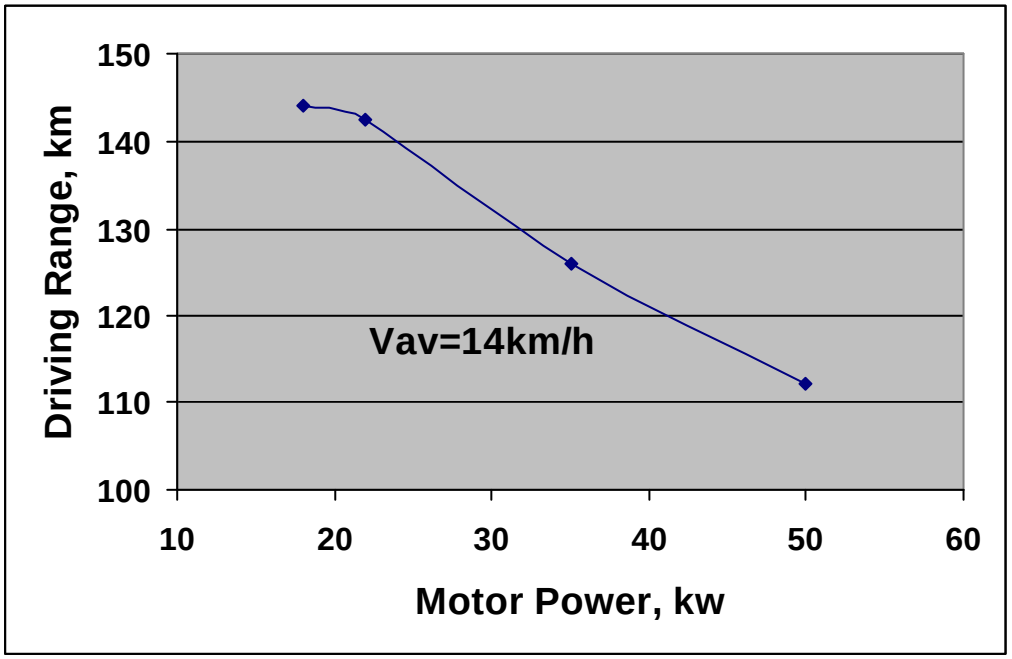

Fig. 21. Motor power effect on driving range, 20 passengers, average velocity 14 km/h.

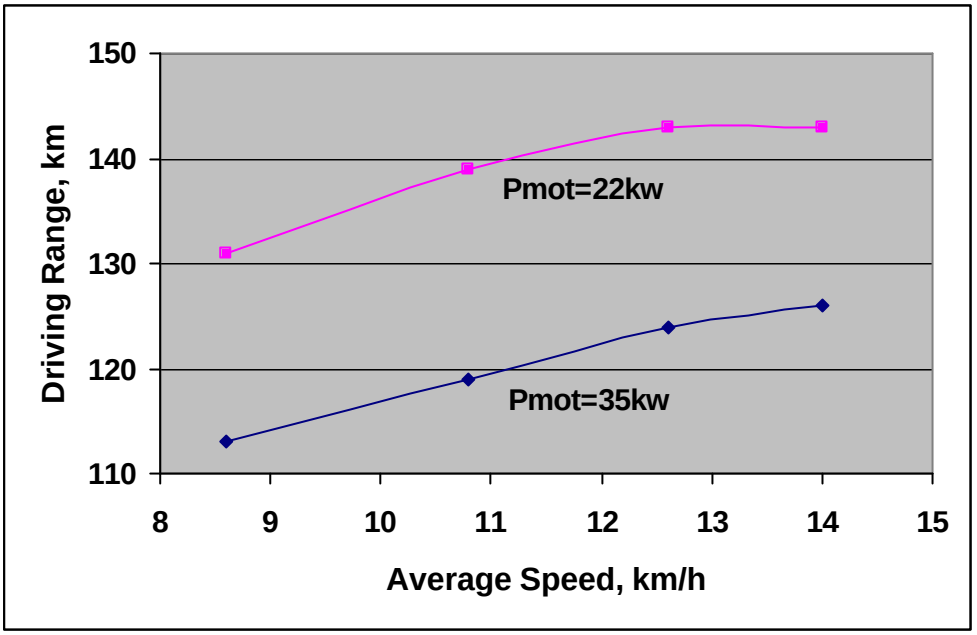

Fig. 22. Effects of average speed and motor power on driving range, 20 passengers.

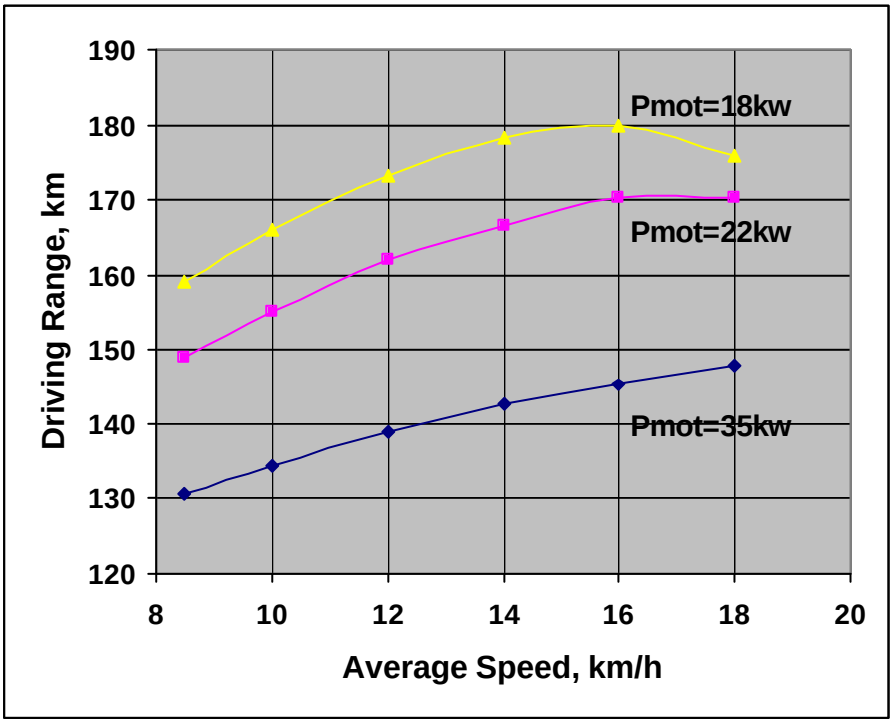

Fig. 23. Effects of average speed and motor power on driving range, 6 passengers.

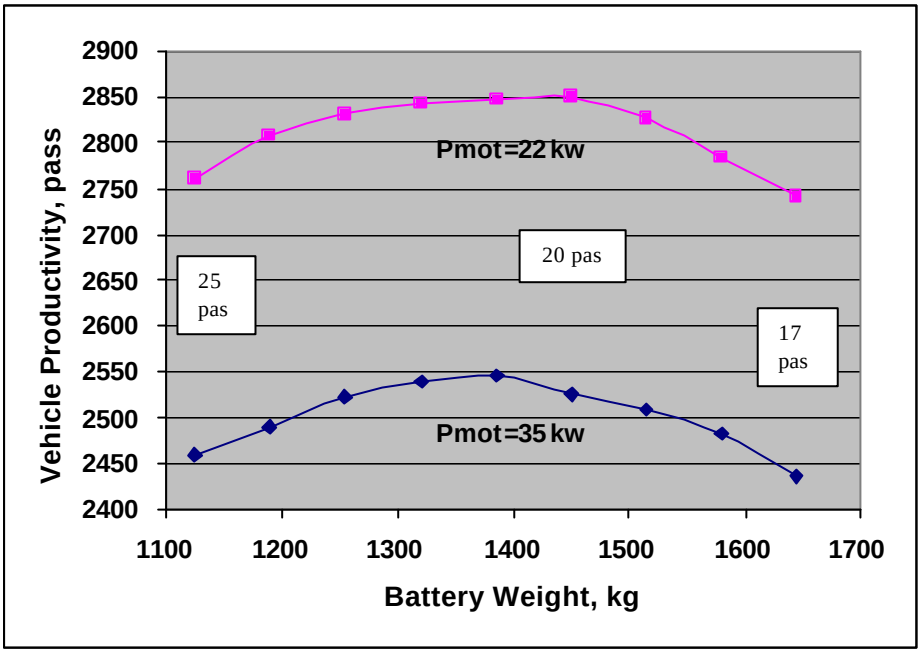

Fig. 24. Effects of battery weight, motor power and passenger number on vehicle productivity, 10 section route, average speed 14km/h.

4.4 ANTIBES ROUTE

4.2.1 Antibes Route: Statistics Analysis

Route

The statistics analysis for the Antibes Route is included in the CyberMove Deliverables D2.3a and D6.2b: Ex-Ante Evaluation Report, [Alessandrini, 2004a], and D2.3b and D4.3: Ex-Post Evaluation Report, [Alessandrini, 2004b]. All the relevant information appears in these reports. The latter reference includes data analysis and simulation results based on the demonstration held in Antibes, in June 2004, as part of the Project, with the FROG cyber car shown in Fig. 8. Three vehicles were used, with 20 passengers' capacity. These two references include all the relevant information. Some highlights of the statistics analysis are presented below, taken from the part of the latter Report, prepared and written by TNO.

The track in Antibes, shown in fig. 9, has a total length of 2989 m, that is about 1.5 km from the station closest to the city center (numbers 6 and 7 in the figure) to the most remote station (numbers 1

and 12). Compared to the Ex-Ante evaluation, the track is extended with 435 m from stations 3 and 10 (parking Vauban) to stations 1 and 12, next to the proposed P+R parking. Also, two more stations have been added at this part of the track. The total number of stations (locations on the track where people can get in or out the cyber cars) is 6. The recharging area is located at the end of the track, near station 1 and 12. In the recharging area is only space for two cyber cars to charge simultaneously (and not three, as suggested by the original drawings). At 4 locations on the track, vehicles may cross the track to enter or leave a parking or gas station. In total, there are 10 crossing lanes. Pedestrians can cross the road at crosswalks. In total, there are 12 crosswalks for pedestrians, of which 6 near stations. In the simulations, the data of vehicle and pedestrian crossings was considered.

The cyber cars always try to drive with the maximum allowed speed. If they drive slower and there is no obstacle or other cyber car within short, they accelerate with the normal acceleration of the real FROG vehicles - of 0.6 m/s^2.

Demand Forecast Estimation

Three periods were considered:
- "May": an average day in May which is considered to be representative for the months January, February, March, May, October, November, December (228 days);
"Salon des Antiquaires": activity with higher demand in April (15 days);
"July": an average day in July with high demand caused by tourist activities, considered to be representative for the months June, July, August and September (122 days).

The demand for these periods is derived from the final demand estimation of the ex-ante evaluation (after iterations), where a free CTS ticket and a system modal share of 23.2 % is considered. In this matrix the total number of people travelling each day by CTS is 957 (hence 1914 one way trips). To get the OD matrices for the periods May, Antiquaires and July we used seasonal factors 0.842, 0.887 and 1.834 respectively.

The average demand is given per 30 minute interval. This is derived from a given hourly distribution of the ex-ante evaluation. The arrivals of the passengers at the stations from which they start their trip are generated by a Poisson-process. All passengers of the CTS are assumed to be arrived by car. Therefore they arrive in groups of people who came with the same car. All people in one group have the same origin and destination and arrival time. The group size is dependent of the period, given by the distributions of Table 5.

Table 5. Distributions of Group Sizes by Period.

	Group size probability		
# persons per group	May	Antiquair	July
1	0.8236	0.8236	0.4816
2	0.155	0.155	0.3175
3	0.0195	0.0195	0.1395
4	0.0018	0.0018	0.046
5	0.0001	0.0001	0.0154
Mean	1.2	1.2	1.8

Some behaviour components are equal for all members of the same group and some may be different for each passenger. Each arriving person pushes a button as soon as he arrives if there are no waiting people yet (the button is pushed by only one person for each arriving group). If not all people can board the first arriving cyber car, one of the remaining people will push the button again. Passengers will get in and out one by one and passengers will get out before passengers will get in. Passengers board in order of their waiting times (longest waiting passengers get in first) and they always board if there is still place in the cyber car (also if groups have to split up). The time for each passenger needed to get in or out the cyber car is normally distributed with mean 2 sec and standard deviation 0.2 sec. This time may be different for each group member.

Comparison specifications of ex-ante evaluation with ex-post simulations

We note the most important similarities and differences between the specifications of the ex-ante evaluation with the ex-post simulations.

The parameter settings of the simulations are based on the parameters of the ex-ante measurements, except where the specifications of the FROG vehicles were different and when different desires where indicated by the concerned people of Antibes. Equal to the ex-ante measurements, the simulations considered 3 cyber cars with a capacity of 20 people. Also, the demand is based on the same O/D matrix, which is adapted for the three periods such that the average equals the demand of the ex-ante measurements. Furthermore, this matrix is also used to estimate the number of trips per O/D pair (extended with two stations). However, some important changes have been implemented in the track layout, speeds and operational hours. These are stated in Table 6.

Table 6. Different settings for ex-ante measurements and ex-post simulations.

	Ex-ante	Ex-post
Operational hours	19 h a day	11.5 h a day
Single length CTS track	1000 m	1450 m
Number of stations	4	6
Number of recharging stations	1	2
Maximum CTS speed	21.6 km/h	20 km/h and 10 km/h
Average car speed	21.6 km/h	< 17.9 km/h
Maximum acceleration	0.9 m/s^2	0.6 m/s^2

CyberMove Simulation Statistics

Table 7 summarizes the main results of the simulation / statistics analysis. All statistics in the table are related to one day, averaged over 100 simulation runs. The yearly figures are calculated from the values of the other periods with weighing factors 228, 15 and 122 respectively. With this weighing, the yearly figures might be a little overestimated since June and September are likely to have a lower demand than July and August, as well as the winter months may have a lower demand than April. In the table, travel times per OD pair are only given for trips which match with the trips in the ex-ante measurements.

The simulation results, (Alessandrini 2004b), include, for all OD pairs: average waiting time of a passenger per station, average in-vehicle time of a trip, average in-vehicle speed of a trip, average

total travel time of a trip (including waiting time), and average speed of a trip (including waiting time).

One interesting finding from the simulations is that the average speed is rather low. Comparing this with normal walking speed, it can be concluded that in this situation, it only rewards in time to go by cyber car from stations 1, 2 and 3 to station 6 at the city center (and back).

Table 7. Antibes Ex-Post Simulation Statistics

Eval Catg	Impact	Indicator		Value May	Value Antiquair	Value July	Yearly figures
Transport patterns	System use	Total passenger·km traveled per day, including walking (discouraged) people		1402	2217	3064	727000
		Total passenger·km traveled per day in peak hours, including walking (discouraged) people		418	690	906	
		Total passenger·km traveled per day in off-peak hours, including walking (discouraged) people		984	1527	2158	
		Total N° of one-way trips, including walking (discouraged) people		1600	2525	3486	828000
		Total N° of one-way trips starting in peak-hours, including walking (discouraged) people		476	784	1025	
		Total N° of one-way trips starting in off- peak-hours, including walking (discouraged) people		1124	1742	2461	
		Average vehicle occupancy over a day per unit of time, excluding recharging time		20.5%	31.5%	41.5%	28.0%
		Average vehicle occupancy per unit of time during peak hours, excluding recharging time		16.5%	26.5%	35.0%	
		Average vehicle occupancy per unit of time during off-peak hours, excluding recharging time		24.0%	36.5%	48.5%	
		Number kilometers empty vehicles over a day		92	81	72	31000
		Number occurrences that a full vehicle cannot accommodate all passengers waiting at a stop		5	43	84	12000
		Total vehicles idle time at “standby point”		2 h 20	1 h 55	1 h 55	33 days
		% discouraged (walking) people		11 %	16 %	19 %	14%
	System performances	Average in-vehicle time of a trip		4 min 40 s	4 min 58 s	5 min 6 s	
		Average in-vehicle time of a trip per OD pair	3-6, 7-10 4-6, 7-9 5-6, 7-8	4 min 59 s 3 min 46 s 2 min 17 s	5 min 8 s 3 min 53 s 2 min 21 s	5 mn 10s 3 mn 55s 2 mn 24s	
		standard deviation in-vehicle time of a trip per OD pair	3-6, 7-10 4-6, 7-9 5-6, 7-8	0 min 16 s 0 min 12 s 0 min 8 s	0 min 15 s 0 min 12 s 0 min 9 s	0 mn 14s 0 mn 11s 0 mn 10s	
		Average total travel time of a trip (incl. waiting time and ‘discouraged people’)		9 min 8 s	10 min 45	11 m 34s	
		Average total travel time of a trip (incl. waiting time and ‘discouraged people’) per OD pair	3-6, 7-10 4-6, 7-9 5-6, 7-8	9 min 39 s 7 min 39 s 8 min 6 s	11 min 42 s 8 min 50 s 9 min 38 s	12 m 53s 9 mn 37s 10 m 30s	
		standard deviation total travel time of a trip per OD pair	3-6, 7-10 4-6, 7-9 5-6, 7-8	4 min 2 s 4 min 44 s 2 min 44 s	4 min 50 s 5 min 31 s 2 min 36 s	6 mn 18s 5 mn 51s 2 mn 25s	
		Average waiting time of a passenger (incl. ‘discouraged people’)		4 min 15 s	5 min 24 s	5 mn 52s	
		Average waiting time of a passenger per station (incl. ‘discouraged people’)	1 2 3 4 5 7	4 m 23s 4 m 22s 4 m 33s 4 m 27s 3 m 11s 4 m 20s	5 min 26 s 5 min 31 s 5 min 44 s 5 min 45 s 3 min 36 s 5 min 34 s	5 mn 13s 5 mn 28s 6 mn 11s 6 mn 21s 3 mn 49s 6 mn 15s	
		standard deviation waiting time of a passenger (incl. ‘discouraged people’)	1 2 3 4 5 7	3 m 42 s 3 m 39 s 3 m 35 s 3 m 16 s 1 m 36 s 3 m 16 s	4 min 12 s 4 min 9 s 4 min 15 s 3 min 35 s 1 min 31 s 3 min 32 s	4 min 3 s 4 mn 14s 4 mn 37s 3 mn 37s 1 mn 25s 3 mn 54s	
		Maximum number of passengers waiting at a stop		25	51	59	
Energy	Energy .consum-ption	Total daily consumption (kWh/day) of all cyber cars		179 kWh	176 kWh	175 kWh	64800 kWh
		Average kW/passenger km		0.128 kWh	0.079 kWh	.057kWh	0.10kWh

Table 8 presents the main results of the ex-ante and ex-post simulations. A detailed description of the results can be found in [Alessandrini, 2004a]. For the purposes of this deliverable, it is noticeable that the energy consumption is much higher in the ex-ante evaluations. This topic will be further discussed in the next section.

Table 8. Different results of ex-ante evaluation and ex-post simulations.

		Ex-ante	Ex-post (average)
Modal share		23.2 %	20 %
Number of trips		411	2270
Vehicle occupancy		11.6 %	28 %
Average in-vehicle time of a trip per OD pair	3-6 4-6 5-6	3 min 2 min 1 min	5 min 3 s 3 min 49 s 2 min 20 s
Weighted average in-vehicle time standard deviation over trips 3-6, 4-6 and 5-6		4.3 s	11.8 s
Average waiting time		1 min 15 s	4 min 50 s
Weighted average waiting time standard deviation		7 s	3 min 27 s
Daily energy consumption		971 kWh	178 kWh
Average kWh/p*km		0.51 kWh/ p*km	0.1 kWh/ p*km

p*km = passenger * km

4.2.2 Antibes Route : Energy Consumption Calculations

Energy consumption calculations have been preformed by three partners of the Project Consortium: TNO, DITS and TRI, by using their own simulation models. They have investigated several aspects of the energy consumption issues. The TNO model is described in the CyberMove Deliverable D2.3b and D4.3: Ex-Post Evaluation Report, [Alessandrini, 2004b]. The DITS model is described in the CyberCars Deliverable D3: New Technologies for Infrastructures, [Immens, 2003]. The TRI model is described in Chapter 2 above. It is noted that the latter is based on simulation of the behaviour of a single vehicle, while the former two simulate not only the CTS energy consumption, but the entire system functioning. The main results of these studies are presented and summarized here.

The TNO and DITS model were employed in the CyberCars and CyberMove Projects mainly for site simulations, and in particular the Antibes Route, where actual operation of CTS's was carried out during the demonstrations in June 2004, within the framework of the Projects. The TRI model was employed here mainly for parametric studies, in order to identify ways to optimize CTS energy consumption and driving range.

A comparison of the TNO and DITS results is presented in Table 9. The differences between the numbers of p*km travelled are mainly due to different approximations: in the TNO simulations, the total energy consumption is 178 kWh and that for per p*km is 0.1 kWh/p*km, thus the total number of daily p*km travelled is 178/0.1 = 1780. If the value of 0.1 kWh/p*km would have been lower, the number of p*km would be larger. For example, if the energy consumed per p*km was precisely 0.095 kWh/p*km,

the value of p*km travelled would be about 1900, thus we can consider that the TNO simulation for p*km travelled is about 2000, similar to the DITS simulation value.

Table 9. Energy Consumption: Comparison of the TNO and DITS Simulations Results

	TNO	DITS
veh*km travelled	318	342
p*km travelled	1780	2028
Average waiting time	4 min 50 s	6 min 50 s
Average occupancy	28%	29.6%
Energy per p*km	0.1 kWh/p*km	0.067 kWh/p*km
Energy per veh*km	0.56 kWh/veh*km	0.396 kWh/veh*km

veh*km = vehicles * km ; p*km = passenger*km

The TRI simulation results for energy consumption and driving range (between rechargings) are presented in Table 10. As can be seen, the values obtained for energy consumption by all the three simulation models (TNO, DITS and TRI) are quite close.

Table 10. Energy Consumption and Driving Range: TRI Simulations Results

Average occupancy	5 pass.	6 pass.
Driving range between rechargings	110	108
p*km travelled between rechargings	550	648
Energy per p*km	0.079 kWh/p*km	0.067 kWh/p*km
Energy per veh*km	0.396 kWh/veh*km	0.404 kWh/veh*km

The TRI simulation model was employed, as mentioned above – for a parametric study, to calculate the energy consumption of the cyber car, for cases of empty and full vehicle. The maximal values of the vehicle speed were taken as 20 and 10 km/h, and maximal accelerations of (deceleration) 1 and 0.6 m/s^2 in the corresponding road sections. Four values of the maximal motor power of the vehicle were considered: 50, 35, 22 and 18 kW. The simulation results are presented in Table 11.

As can be seen from the Table, E_{cons} for motor power of 22 kW is lower by about 20% than that for the P_{max} of 50 kW for an empty vehicle and by about 10% for a fully loaded vehicle. The effect can be explained by the increase of the motor efficiency with the decrease of the traction power.

It is noted that there are no energy consumption and driving range values listed in Table 11 for the low motor power - 18 kW, and vehicle with full capacity. The reason for this is the lack of enough power to propel the vehicle at the maximal stipulated acceleration in the case.

Table 11**.** Energy Consumption: TRI Simulation Results.

Pmax, kW	Energy Consumption per km, kWh/km		Driving Range, km	
	Empty	Full Load	Empty	Full Load
50	0.460	0.563	91	75
35	0.406	0.511	105	84
22	0.364	0.509	119	86
18	0.362	---------	120	----------

It is emphasized, again, that the motor power can be optimized, based on pre-designed acceleration and speed values, i.e. desired driving pattern.

Fig. 25 shows the effects of the battery weight and the average speed on the vehicle productivity (number of passengers moved). It is observed, again, that there is a maximum for certain values of these parameters, so it is possible to design the system for optimized energy consumption.

It is interesting to note that unlike the behaviour of the curves for the Rivium – 2 case (Chapter 4.3). Here, for the Antibes case, the vehicle productivity decreases with the increases of the average speed. This is due to the rather large number of stops and of pedestrian crossings, so that there are many speed changes and accelerations that require more energy.

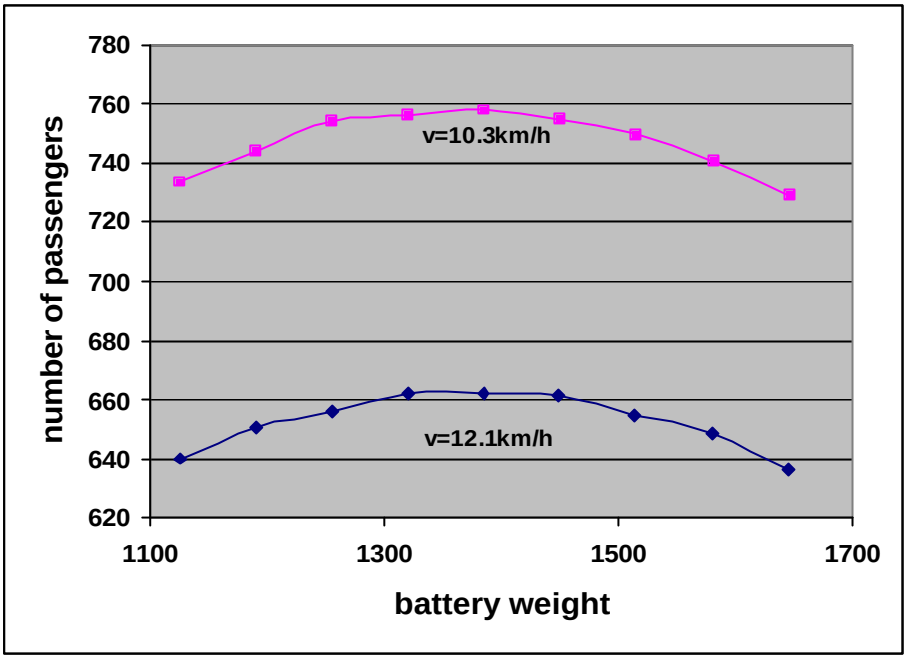

Fig. 25. Effects of battery weight and average speed on number of passengers moved.

5. SUMMARY

This document presents the work conducted within the framework of WP4 of the CyberMove Project: "Data Collection and Analysis". Algorithms and models were developed by TNO, DITS and TRI to simulate the behaviour of a cyber car on the road and a cybernetic transportation system (CTS). The TNO and DITS model were employed for site simulations, and in particular the Antibes Route, where actual operation of CTS's was carried out during demonstrations in June 2004. The statistics analysis for the Antibes appear in the CyberMove Deliverables D2.3a and D6.2b: Ex-Ante Evaluation Report, [Alessandrini, 2004a], and D2.3b and D4.3: Ex-Post Evaluation Report, [Alessandrini, 2004b], some of the main results are summarized in the present Deliverable, including demand patterns. The TRI model was employed here mainly for parametric studies, in order to identify ways to optimize CTS energy consumption and driving range.

A theoretical model for simulating the performance of cybercars was developed, in order to calculate the energy consumption of the vehicle and the CTS. Collected data and simulation results of several cybercars and driving patterns are presented for four sites: INRIA Test Site, Technion Campus, RIVIUM–2 Loop and Antibes Route. The results obtained for any system under design can be used for comparison between various options of the vehicles power train and its optimization. This enables to select its optimal components, like rated (or maximal) motor power, battery weight, etc. The results include daily energy consumption and recovery (by regeneration during braking) of the vehicles for the four sites mentioned above, and parametric studies of the effects of various vehicle and driving pattern data. Statistics analysis, calculations of daily energy consumption in dependence of season and comparison of ex-ante evaluation with ex-post simulations, which differ by CTS track length, number of stations, maximal and average car speed and acceleration for the Antibes site are presented. The energy impact is discussed, based on the evaluation of the results.

The main conclusion emerging from the simulation results is, indeed, that the CTS energy consumption can be minimized by careful design and selection of optimal parameters of both the vehicle and the driving pattern. It has been demonstrated that the functions of energy consumption, driving range and vehicle (or system) productivity (or number of passengers moved) have extrema at certain values of the battery weight, the maximal (or rated) motor power and the average vehicle speed (which represent the driving pattern, i.e. accelerations / decelerations). The importance of regenerative braking for energy conservation and increase of the driving range is also depicted.

The results clearly show that it is possible to design the CTS and its operational procedure such as to offer better service and to minimize energy consumption. It is possible to develop a method for the selection of components for optimal system operation. There are numerical tools – optimization softwares – available for it, of various level of sophistication. Since there are several parameters involved, it is necessary to use a multi-parameter (multi-dimension) code. Moreover, it might be required to quantify some parameters and devise weighting factors to take into account waiting times, charging equipment and costs in general.

The work described in this Report has been carried out by the Consortium partners: TRI, INRIA, YME, FROG, TNO and DITS.

REFERENCES

Alessandrini, A. 2004a. Ex- Ante Evaluation Report. CyberMove Deliverable D2.3a and D6.2b.

Alessandrini, A. 2004b. Ex- Post Evaluation Report. CyberMove Deliverable D2.3b and D4.3.

Bekhor, S. and Zvirin, Y, 2004. Estimating the Potential Use of Cybernetic Cars for a University Campus. Paper presented at the 10th World Conference in Transport Research, Istanbul, Turkey.

Bosch, G. 1996. Automotive Handbook, 4-th edition, SAE Society of Automotive Engineers, Warrendale, PA USA.

Caraceni, A. Cipolla, G. & Barbiero, R. 1998. Hybrid Power Unit Development for Fiat Multipla Vehicle, 981124, Society of Automotive Engineers.

Ehsani, M., Yimin, G. & Buttler, L. 1999K. Design Optimization of Electrically Peaking Hybrid Vehicles, Texas A&M University, Advanced Vehicles System Research Program, College Station, TX 77843-3128.

Harats, Y., Koretz, Y., Goldstein, B. J. & Korall, M. 1995. The Electric Fuel System Solution for Electric Vehicles. Presented at "Batteries und Batteriemanagement" Conf. Essen, Germany.

Hochgraf, C. G., Ryan, M. J. & Wiegman, H. L. 1996. Engine Control strategy for a series Hybrid Electric Vehicle Incorporating Load Levelling and Computer Controlled Energy Management, SAE 960230.

Immens A. 2003. New Technologies for Infrastructures. CyberCars Deliverable D3.

Kottick, D., Tartakovsky, L. Gutman, M. & Zvirin Y. 2000. Results of electric vehicle demonstration program. Proceedings IEEE Conference, Tel-Aviv, 318 – 321.

Meier-Engel, K. 2000. Failure Time and Energy Consumption of Vehicles. Matador Contract Report JOE3-CT97-0081.

Nicol, B. D. & Rand, D. A. J. 1984. Power Sources for Electric Vehicles, Elsevier.

SIMPLEV, 2000. SIMPLEV, Simulating Electric&Hybrid Vehicles,
http://ev.inel.gov/simplev/pg2.html